December 21, 2024

REDSHIFT AND THE SHAPE OF THE UNIVERSE

Nathan Burwig[1], Maxwell Kaye[2] and Krzysztof Sliwa

Tufts University

Department of Physics and Astronomy
Medford, Massachusetts 02155 USA

Abstract

Hubble's observation in 1929 that redshifts of far-away objects increase with their distance is customarily interpreted as being due to expansion of the universe, leading to the widely accepted theory of the Big Bang and a spatially flat, infinite universe. We explore an alternative model of the universe, proposed by Segal in 1972, which has geometry $\mathbb{R} \times \mathrm{S}^3$. It is eternal, not expanding, and is spatially curved, compact and finite, as in the Einstein static universe. Our preliminary analysis of open source datasets demonstrates that the model's predictions are consistent with two important types of cosmological data: cosmological redshift and cosmic background radiation. With new data from the James Webb Space Telescope, verification of predictions that distinguish the standard model from Segal's model of the universe is increasingly feasible.

[1]now at Arizona State University, Tempe, Arizona, USA
[2]now at McGill University, Department of Mathematics and Statistics, Montreal, Canada

INTRODUCTION

In 1929, Hubble [1] showed that the redshift in the light spectra of distant nebulae is proportional to their distances from Earth. Hubble suggested that this cosmological redshift could be analogous to the familiar Doppler effect, except not caused by sources moving away from each other in space, but by the stretching of the space itself, if the universe is expanding like in the de Sitter solution to Einstein's general theory of relativity. In 1935, Hubble and Tolman [2] considered the expansion of the universe as one possible explanation for the redshift-distance relation observed by Hubble. They also mentioned a possibility that the increase of redshift with distance could be caused by some other unknown effect due to the geometry of the universe. However, no definitive explanation of this kind was found at the time, and the expanding universe hypothesis became accepted as fact.

In the Lambda Cold Dark Matter Model (ΛCDM), also known as the Standard Cosmological Model (SCM), the shape of the universe is assumed to be spatially flat, $M_0 = \mathbb{R} \times \mathbb{R}^3$. In 1972, Irving Segal proposed an alternative explanation for the observed increase of redshifts with the distance of far-away objects [3]. The axioms of physical symmetries—global isotropy and homogeneity of space and time, and its causality properties, are satisfied not only by Minkowski spacetime, $\mathbb{R} \times \mathbb{R}^3$, but also by a universe whose geometry is $\mathbb{R} \times \mathrm{S}^3$. It is the geometry of the Einstein static universe - non-expanding, spatially closed, finite, and eternal. Einstein abandoned this model after the increase of redshift with distance became accepted as evidence for expansion of the universe. The two geometries are indistinguishable locally, even across intergalactic distances, with observable differences appearing only on cosmological scales.

The two universe geometries and their causal structures are deeply connected, and their relationship gives rise to possibly observable differences. Not only is $\mathbb{R} \times \mathbb{R}^3$ the tangent space to each observer in $\mathbb{R} \times \mathrm{S}^3$, but Minkowski space can be causally embedded in Segal's universe [13] . This means that, for any observer in $\mathbb{R} \times \mathrm{S}^3$, stereographic projection onto Minkowski space tangent to that observer's location preserves the time-orientation of all observable sequences of events. Segal postulates that observations are indeed made in this local Minkowski projection, and from this hypothesis, shows that redshift arises naturally. This theory provides a verifiable prediction for the dependence of this geometric redshift on the geodesic distance light travels through in $\mathbb{R} \times \mathrm{S}^3$, which is distinct from the redshift-distance relation provided by the ΛCDM theory.

A concise introductory overview of Segal's theory was given by Daigneault and Sangalli [4]. A detailed review of Segal's book [13] was written by Taub [5]. References to Segal's papers and books on Chronometric

Cosmology can be found in the bibliography[3,6-34].

Segal's work was not accepted by his contemporaries. They raised both theoretical and empirical concerns about chronometric cosmology [16, 25], which Segal addressed [17, 26], but the conversation died out. In the modern day, with newly available data that is more precise and farther reaching, we seek to reopen the question of chronometric cosmology and consider if it can be falsified in the modern context. Surprisingly, the currently available data does not falsify Segal's model.

We begin by providing a brief review of theoretical background for Segal's theory (section 1), and then present our comparison of open-source observational redshift and CMB data with both cosmological models (section 2).

1 Segal's Chronometric cosmology

1.1 Motivation

Segal's original motivation was to explore possible generalizations of Minkowski space-time of special relativity to some other 4-dimensional manifold, given that Maxwell's equations are not only Lorentz invariant but also conformally invariant. The Poincaré group and Minkowski space-time would then be a limiting case of a more accurate theory, similarly to the Galilean group being a limit of the Lorentz group when the speed of light approaches infinity.

The most natural generalization of Minkowski space-time of special relativity would be a 4-dimensional manifold which is not only Lorentz invariant, but also conformally invariant. The group $\mathrm{SO}(2,4)$ is the 15-parameter conformal group of Minkowski space-time. (Sometimes its double cover $\mathrm{SU}(2,2)$, which is locally isomorphic to $\mathrm{SO}(2,4)$, is chosen). The Lie Algebra $\mathrm{so}(2,4)$ is composed of 10 Poincare generators, $M_{\mu\nu}$ (space rotations and boosts) and P_μ (translations), together with scale transformation D and special conformal generators K_μ. By a theorem by Alexandrov and Zeeman [36], causality preserving transformations on Minkowski space are conformal transformations.

Lie algebras of pseudo-orthogonal groups $\mathrm{O}(1,5), \mathrm{O}(2,4)$, and $\mathrm{O}(3,3)$ are deformable into that of the fundamental dynamical variables (momenta, boosts, and space-time coordinates) in relativistic quantum mechanics [6] . As pointed out by Segal [7], $\mathrm{O}(1,5)$ which is the group of de Sitter space, is difficult to reconcile with the principle of positivity of energy in quantum mechanics, as it does not have a self-adjoint generator corresponding

to a nonnegative energy in any nontrivial unitary representation. The group $\mathrm{O}(2,4)$, the conformal group of Minkowski space, is a candidate for a more accurate higher symmetry group as it is free from this deficiency. In 1971, Segal suggested that the acausality of conformal spacetime could be remedied by its replacement with the locally identical universal covering space [8].

1.2 Postulates

Segal's cosmology [13] is derived from the following assumptions:

- space-time is a 4-dimensional manifold
- space-time has causal structure: (a) at each point in the universe there exist a convex cone of infinitesimal future directions in the tangent space to the manifold at that point; (b) there are no closed timelike loops
- space-time is causally spatially isotropic—at any point of spacetime there is no preferred spacelike direction (this assumption does not imply spatial uniformity in the distribution of matter)
- space-time is causally temporally isotropic—there is no preferred timelike direction at any point of space-time. For any two timelike directions at a given point of spacetime, there is a causal diffeomorphism of spacetime onto itself that maps one of these directions on the other
- spacetime can be globally factorized into $time \times space$
- spacetime is causally temporarily homogenous: translations with respect to the $time \times space$ factorization form a group of causal automorphisms of spacetime, the temporal group belonging to this factorization; the energy is invariant under a group of *causal* temporal translations related to a factorization of spacetime as $time \times space$
- spacetime is spatially homogenous

Segal showed [13] that these axioms are satisfied by only two possible manifolds: Minkowski $M_0 = \mathbb{R} \times \mathbb{R}^3$ and $M = \mathbb{R} \times \mathrm{S}^3$.

1.3 Compactification of Minkowski space

Segal discussed compactification of Minkowski space in two ways: as a projective quadric in 6-dimensional real space of signature $(2,4)$; or as a manifold with a $\mathrm{U}(2)$ group action, which leads to a generalization of

stereographic projection. More information about the mathematical details can be found in Appendix 1.

1.4 Segal's cosmological redshift

Minkowski space M_0 can be thought of as the tangent space at any point of $\mathbb{R} \times \mathrm{S}^3$, just as the complex plane is tangent to the Riemann sphere.

However, the mapping between the M_0 and $\mathbb{R} \times \mathrm{S}^3$ spaces is non-linear, therefore the time coordinate measured in M_0 depends on both the time and space coordinates in $\mathbb{R} \times \mathrm{S}^3$. Thus time and energy differ crucially in the two models [13]. Local observations of dynamical quantities are represented not necessarily by generators of true, global symmetries, but by generators of corresponding symmetries in the flat tangential space. While angular momenta remain unchanged, energy and linear momenta differ. The true energy is no longer represented by $-\mathrm{i}\hbar\frac{\partial}{\partial t}$, but by an operator $-\mathrm{i}\hbar\frac{\partial}{\partial \tau}$ where τ is the global time.

Assuming that the global, physical time τ is that derived from the $\mathbb{R} \times \mathrm{S}^3$ factorization, and that Minkowski time t is only a local projection of it, the redshift of photons propagated over large distances is obtained from the conformal invariance of Maxwell's equations and the requirement that the action of the time evolution groups, both standard (Minkowski) and non-standard ($\mathbb{R} \times \mathrm{S}^3$), is unitary. The global time τ and Minkowski time t coordinates are related by the equation [13]

$$t = \frac{2R}{c}\tan\left(\frac{c\tau}{2R}\right) \tag{1}$$

where R is the radius of a 4-dimensional ball whose boundary S^3 constitutes our 3-dimensional space, and c is the speed of light. The two times correspond to two concepts of energy. The global, cosmic energy in $\mathbb{R} \times \mathrm{S}^3$ is conserved, while the photon energy measured in Minkowski $\mathbb{R} \times \mathbb{R}^3$ is reduced by the redshift. The redshift-distance relation in Segal's model [13] constitutes a verifiable prediction of the dependence of this redshift z on the geodesic distance $l = c\tau$ on S^3

$$z = \tan^2\left(\frac{c\tau}{2R}\right) = \tan^2\left(\frac{\rho}{2}\right). \tag{2}$$

The dimensionless quantity $\rho = l/R$, or a 4-dimensional analogue of the polar angle, runs from 0 to π when light is traveling from the emission point to its antipode in S^3. The redshift becomes infinite when the light goes around through a half-turn around the $\mathbb{R} \times \mathrm{S}^3$ universe to the observer. The redshift-distance relation can be also derived geometrically [28].

1.5 Segal's cosmology: matter and interactions

In the $\mathbb{R} \times \mathrm{S}^3$ space-time, Maxwell's equations remain intact, as they are conformally invariant. The solutions to Maxwell's equations in Minkowski space extend uniquely to their solutions in the $\mathbb{R} \times \mathrm{S}^3$ universe [23]. The same holds for the Dirac equation, and for the Yang-Mills equations, which describe fermions and the strong and weak interactions in particle physics. These equations are conformally invariant in absence of matter which allows to relate the Dirac and Yang-Mills theories on Minkowski space-time with their analogues on a manifold with the boundary.

Einstein's general relativity relates gravitation to curvature of space. In Einstein's original equations, flat Minkowski space is the simplest solution to the vacuum field equations of an empty universe. Einstein's modified equations include a cosmological constant term introduced to allow for a non-expanding universe in the presence of matter. However, the modified equations are the most general equations satisfying the usual minimal conditions. They allow for an empty space to have curvature, as in Segal's model. The inclusion of this term does not result in any inconsistencies with General Relativity. The relation of Segal's universe to general relativity is analogous to that for special relativity, except that the geometry of empty space is $\mathbb{R} \times \mathrm{S}^3$ rather than $\mathbb{R} \times \mathbb{R}^3$. In the limit of $R \to \infty$, the $M = \mathbb{R} \times \mathrm{S}^3$ universe becomes Minkowski $M_0 = \mathbb{R} \times \mathbb{R}^3$ spacetime. Segal's theory does not assume general relativity, but is compatible with it [13].

To quote Segal himself [19]: "How is general relativity and its relation to cosmology affected? The postulated infinitesimal structure of space-time in general relativity, i.e. of reference or empty space-time, is changed from a Minkowski space, formed from the tangent space at the point of observation, to a chronometric space, $\mathbb{R} \times \mathrm{S}^3$, invariantly attached to the point as the universal covering space of the conformal compactification of the tangent space with respect to the metric given in it. As far as is now known, the radius of the S^3 is too large (in conventional units; in natural units the S^3 is of unit radius) to produce any presently observable effects in the small, and local observable aspects of general relativity are therefore unaffected. In the large, because of the compactness of S^3 it is necessary, as Einstein proposed, to add the cosmological term to his equation. Overall, the resulting universe departs widely from the Friedman-Lemâitre model—any expansion, if present at all, must be slight-but in its gross features is consistent with Einstein's original static conception."

2 Comparison of models of universe with data

The predicted redshift-distance relations are different in Segal's model and in the expansionary SCM model [37,38]. At least in principle, the data can differentiate between the two models, leading Segal to publish several papers analyzing the data available at his time. However, since his passing in 1998, enormous progress has been made in observational astronomy. Modern galactic surveys are covering larger areas of the sky and and provide data from greater redshifts than have been probed previously. Here, we set out to investigate whether Segal's model can be falsified with modern data.

2.1 The magnitude-redshift relation

For distant objects, distance is not a directly observable quantity, and it can only be estimated by using various proxies, such as magnitude. If one assumes that the objects are 'standard candles' with the same absolute luminosity, the purely geometric relations between apparent luminosity and distance allows comparison of correlations between the observed magnitude and redshift, $m(z)$. The data for type 1a supernovae, the best known 'standard candles', agrees very well with the SCM, but it also agrees with Segal's model. In Figure 1, the data from the Supernova Cosmology Project [39] compilation 'Union2.1' is shown along with theoretical predictions from the SCM (red) and from Segal's $\mathbb{R} \times \mathrm{S}^3$ cosmology (green). More information about the theoretical predictions used, and the fits themselves can be found in Appendix 2.

One should keep in mind that the comparison, although in principle very simple, is not trivial due to possible but unknown effects of extinction of light from distant sources and details of star evolution in time.

2.2 The number count $N(< z)$ relation

Another independent observable is the 'number count', or the number of objects of a given type seen in a fixed cone versus their redshift, $N(< z)$. Assuming a uniform distribution of objects in the universe, $N(< z)$ is directly proportional to the volume, $V(< z)$, enclosed in this cone, and is thus sensitive to the geometry of space. Plotting $N(< z)/N(< z_{max})$, where z_{max} is the maximum redshift in a sample, and comparing it to $V(< z)/V(< z_{max})$ as a function of redshift z can, in principle, differentiate between possible geometries of the universe.

The data from several ASTRODEEP Frontier Fields [40], based on a combination of observations from the Hubble Space Telescope, the Spitzer telescope, and the ground-based VLT Hawk-I is found to be in agreement

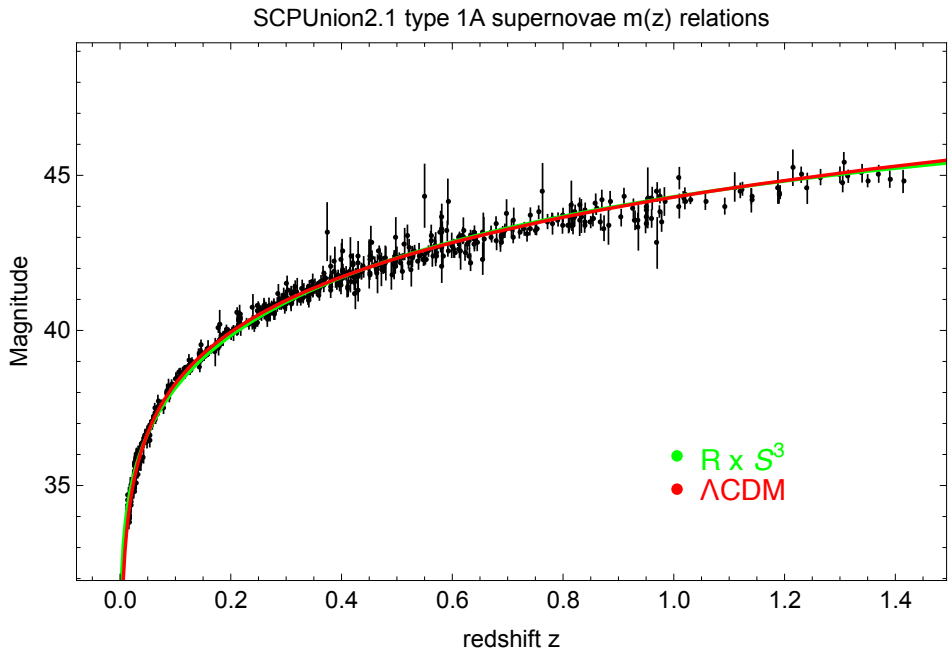

Figure 1: The SCP 'Union2.1' SN Ia dataset is an update of the 'Union2' compilation. Plotted are observed magnitudes as a function of redshift for 580 SNe type Ia that pass usability cuts. The red curve s the result of fits based on the Standard Cosmological Model [37] of $m(z)$ within SCM with $q_o = 1/2$ for a flat space, and including a correction for possible light extinction. The green curve is based on Segal's model $\mathbb{R} \times \mathrm{S}^3$. The prediction from Segal's model also includes a correction for the observed intensity to account for possible extinction, $I_{corr} = I\ \exp(-\lambda c\tau)$, corresponding to the extinction length of $1/\lambda \approx \frac{1}{2}R$, the radius of the universe. The two fits have the same number of free parameters. Fits to a newer parametrization [38], assuming zero curvature term $\Omega_k = 0$, and taking $\Omega_{matter} = 0.276$ for the matter term (red), as determined independently from the CMB studies, gives virtually identical results to those obtained with the SCM parametrization used in the fit [37].

with predictions of Segal's model. In Figure 2, we show results on $N(< z)$ as a function of the redshift z for the ASTRODEEP Abell-2744 and MACS-J0416 fields, and in Figure 3 we show the magnitude-redshift relations, $m(z)$, based on the same data, for completeness. We selected only those objects in the ASTRODEEP Abell-2744 and MACS-J0416 fields that have redshifts determined spectroscopically, or photometrically with the redshift uncertainty range ZBEST_SIQR < 0.1. In Figure 4, we show results on $N(< z)$ as a function of the redshift z for the ASTRODEEP Abell-2744 and MACS-J0416 fields only for objects that have redshift determined spectroscopically.

One should keep in mind that such comparisons may be affected by selection biases, by the unknown effects of extinction of light when it travels through distant parts of the universe, and by possible effects due to evolution of galaxies in time. For very large redshifts, there should be no galaxies in the SCM, as they need some minimum time to form after the Big Bang.

Interestingly, several recent papers based on data obtained with the James Webb Space Telescope [41], reported observations of distant galaxies of uncharacteristically large mass, given their high redshifts [42, 43]. According to the current ideas about evolution of galaxies in the expanding universe, such objects are not expected so early after the Big Bang. However, the presence of galaxies this large at such high redshifts is consistent with a static $\mathbb{R} \times \mathrm{S}^3$ universe, in which galaxies are distributed homogenously in the S^3 space, including distances corresponding to very large redshift values.

2.3 The cosmic microwave radiation

It is an important observational fact that our universe is filled with omnidirectional cosmic microwave background radiation (CMB) with the black body spectrum corresponding to temperature of approximately $T = 2.7\ K$. In the ΛCDM model, the CMB is explained as the light that was originally emitted from 'the surface of last scattering' about 380,000 years after the Big Bang; now at redshift of $z \sim$1100 [44].

In Segal's model the CMB corresponds to 'residual light' , light that has not been absorbed over multiple turns around the spatially closed $\mathbb{R} \times \mathrm{S}^3$ universe. Segal showed that its energy distribution is expected to be the Planck black-body spectrum [23]. The only properties of light required in the proof are that it is described by Maxwell's equations, Bose-Einstein statistics, and that it is stochastically emitted and absorbed by matter via a temporally invariant interaction over many turns around the $M = \mathbb{R} \times \mathrm{S}^3$ universe.

As light takes several turns about this closed universe, the absorption coefficient α characterizes the amount

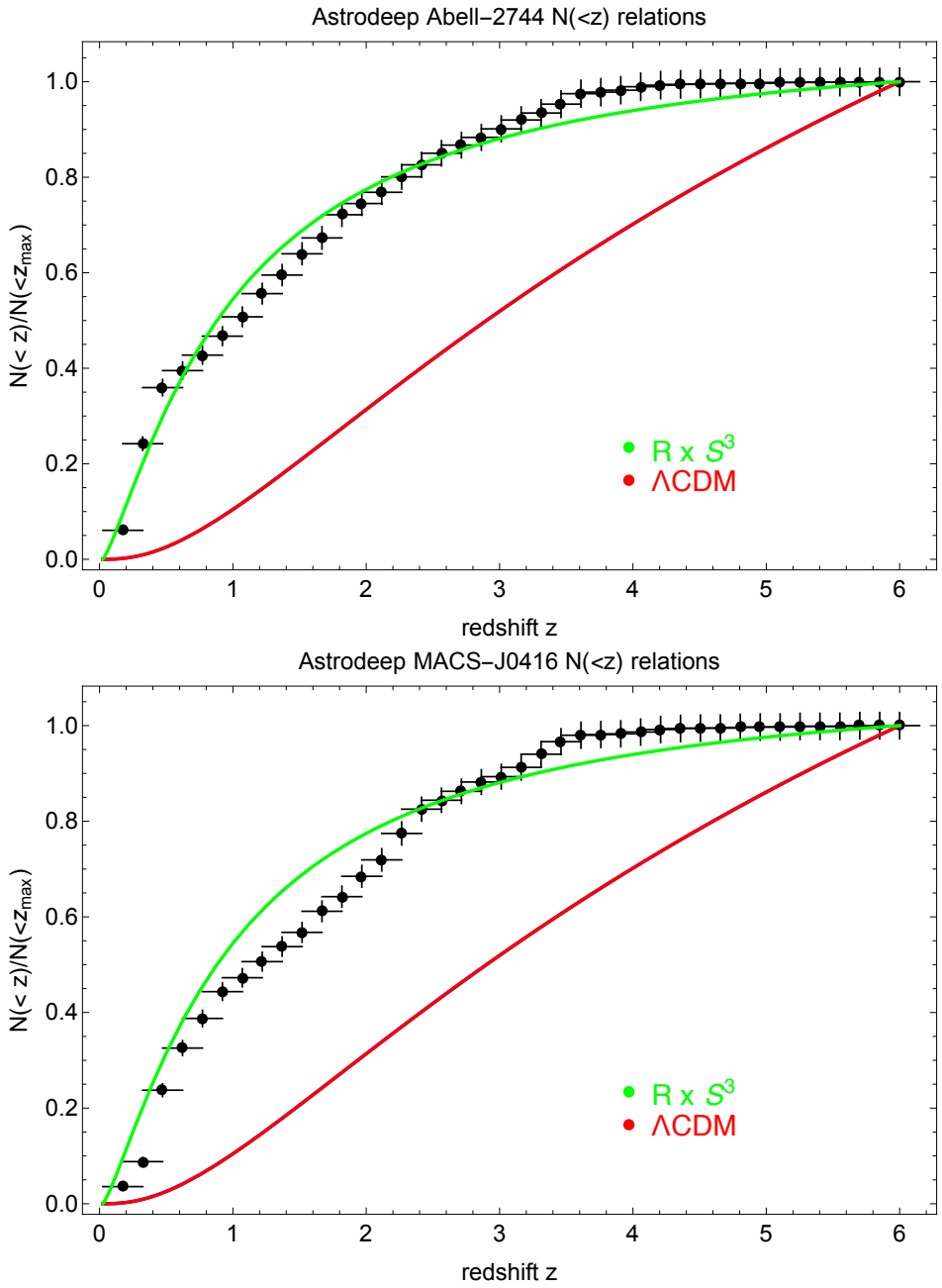

Figure 2: The normalized number count, $N(<z)/N(<z_{max})$ based on data from two ASTRODEEP Frontier Fields, Abell-A2744 and MACS-J0416, for objects that have their redshifts measured spectroscopically, or photometrically with the redshift uncertainty range ZBEST_SIQR < 0.1. The curves are the normalized volumes as a function of redshift z, $V(<z)/V(<z_{max})$ calculated for SCM (red) and Segal's $\mathbb{R} \times \mathrm{S}^3$ cosmology (green). The number count $N(<z)$ is proportional to the volume, $V(<z)$, enclosed in a chosen angular cone up to redshift z. The dependence of the volume contained within redshift z is $V(<z) \sim (1 - \frac{1}{\sqrt{1+z}})^3$ for SCM [37], and $V(<z) \sim \tan^{-1}\sqrt{z} - \frac{1}{4}\sin\left(4\tan^{-1}\sqrt{z}\right)$ for Segal's model [13], correspondingly.

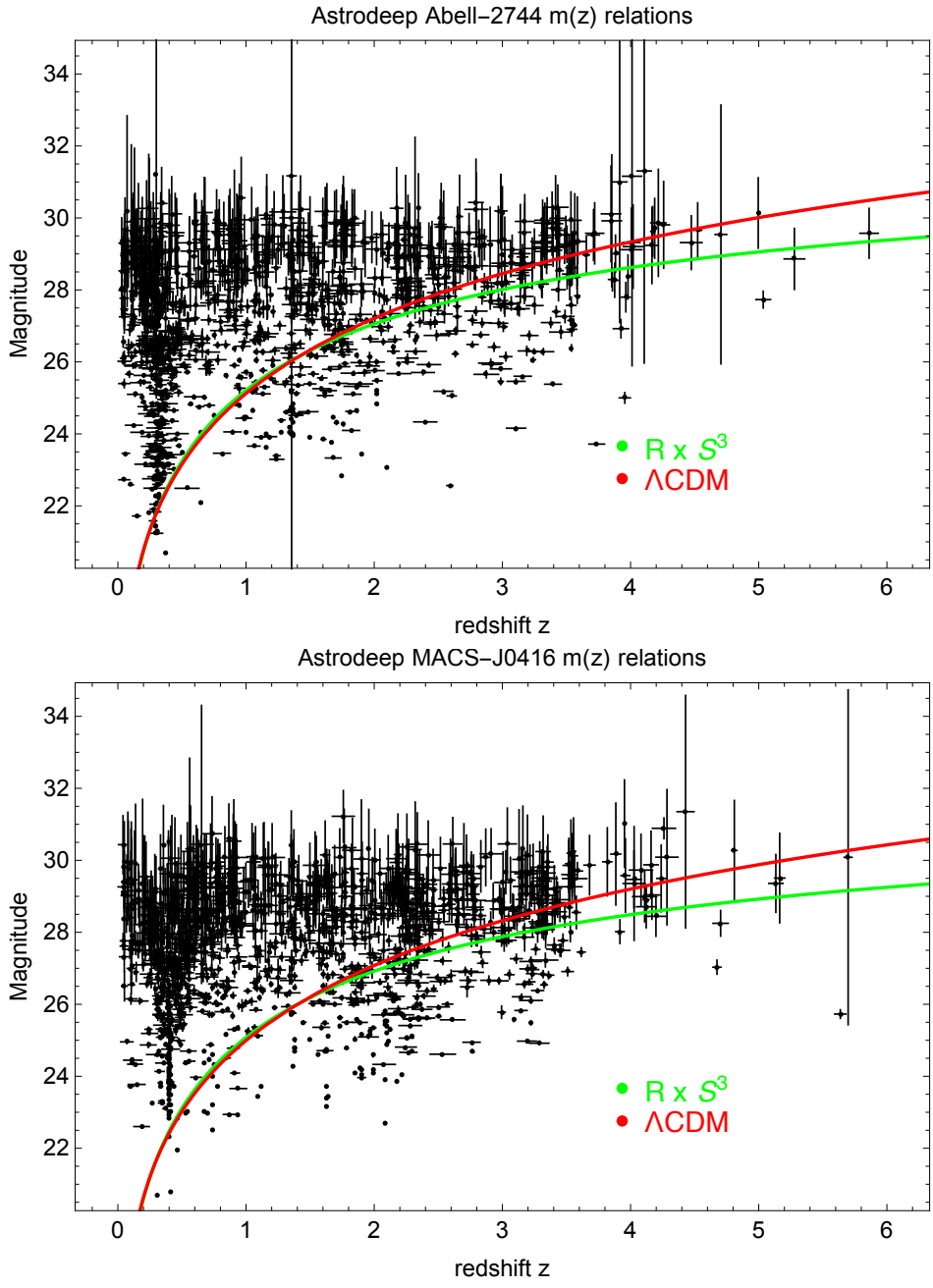

Figure 3: The observed magnitude as a function of redshift for objects from two ASTRODEEP Frontier Fields, Abell-2744 and MACS-J0416, for objects that have their redshifts measured spectroscopically, or photometrically with the redshift uncertainty range $ZBEST\_SIQR < 0.1$. The curves shown are results of fits based on Standard Cosmological Model [37] (red) and Segal's $\mathbb{R} \times \mathrm{S}^3$ (green), using the same parameters as obtained in fits to the SCP 'Union2.1' supernovae data shown in Figure 1, except for an additive constant.

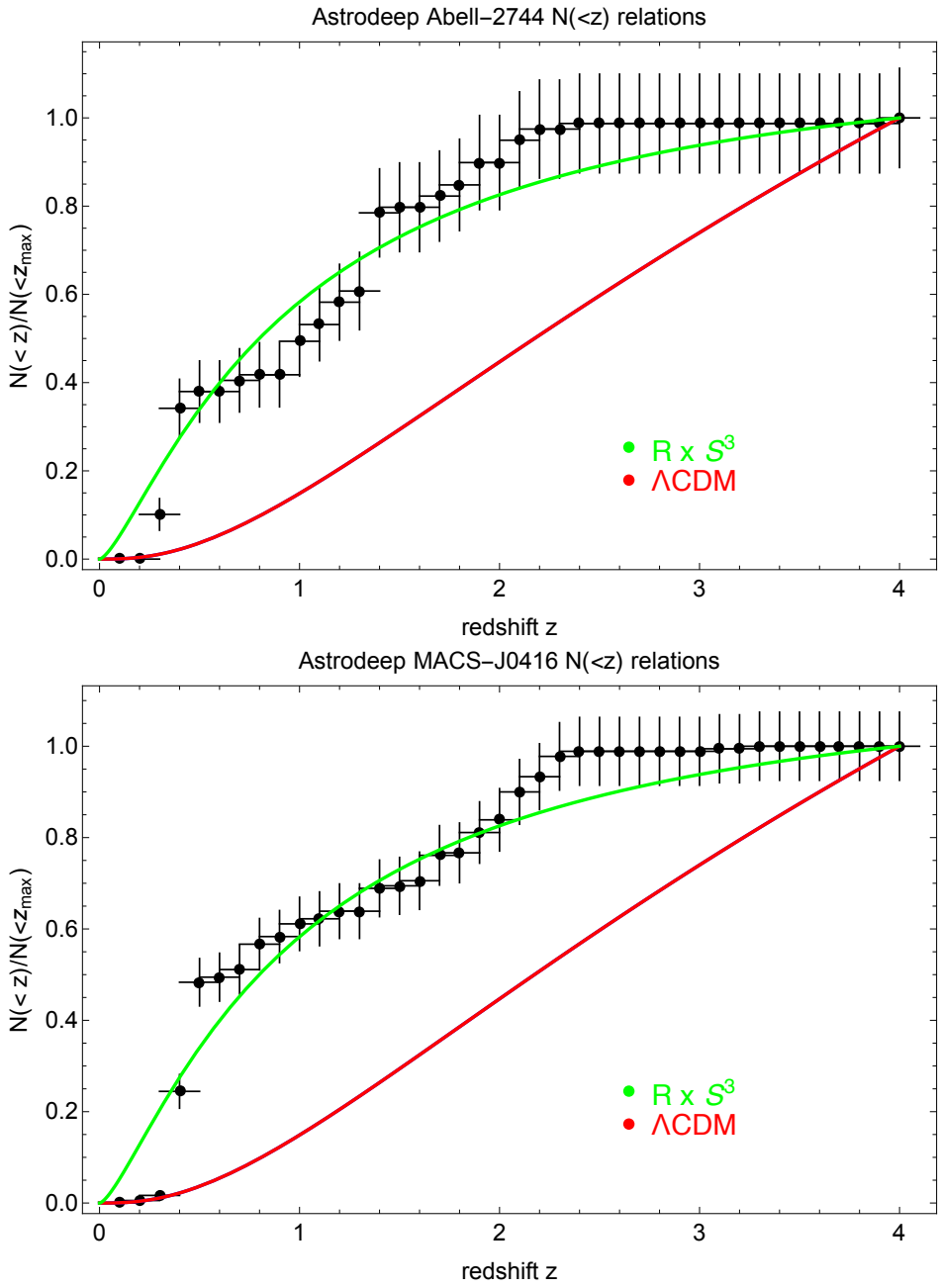

Figure 4: The normalized number count, $N(<z)/N(<z_{max})$ based on data from two ASTRODEEP Frontier Fields, Abell-A2744 and MACS-J0416, for objects that have their redshifts measured spectroscopically. The curves are the normalized volumes as a function of redshift z, $V(<z)/V(<z_{max})$ calculated for SCM (red) and Segal's $\mathbb{R} \times \mathrm{S}^3$ cosmology (green). The number count $N(<z)$ is proportional to the volume, $V(<z)$, enclosed in a chosen angular cone up to redshift z. The dependence of the volume contained within redshift z is $V(<z) \sim (1-\frac{1}{\sqrt{1+z}})^3$ for SCM [37], and $V(<z) \sim \tan^{-1}\sqrt{z} - \frac{1}{4}\sin\left(4\tan^{-1}\sqrt{z}\right)$ for Segal's model [13], correspondingly.

of light absorbed in one half turn around the manifold. In Segal's simplest model, light is absorbed by matter present in N galaxies represented by black disks of radius r. The absorption coefficient α per single half-turn around the universe is closely related to the fraction of the celestial sphere obscured by galaxies distributed uniformly in a closed S^3 space. Since the number of galaxies in the compact S^3 is finite, $\alpha \ll 1$. The total energy flux of light that has not been absorbed over n half-turns is $P\mathrm{e}^{-\alpha n}$, where P is the energy flux of 'pristine' light that did not yet travel by more than a half-turn around the universe. Summing a resulting power series over multiple half-turns around the universe gives

$$P_{\mathrm{CMB}} = \sum_{n=1}^{\infty} P\mathrm{e}^{-\alpha n} = P/\alpha \tag{3}$$

since $\alpha \ll 1$. P is the energy flux of 'pristine' light, emitted by N galaxies distributed uniformly in the universe, averaged over the entire universe and taking redshift into account. We calculated the average energy flux P following a geometrical analysis analogous to an estimate of the absorption coefficient α. The 'pristine' light originates as light emitted by N galaxies, represented by disks of radius r and all of the same typical luminosity. In this model, the number of galaxies N, their radii r, and the radius of the 4-D hypersphere R, cancel out. More information about the theoretical predictions used can be found in Appendix 3. As a result, one can express P_{CMB} in terms of the energy flux of light emitted by a typical galaxy at some distance from Earth, in terms of the radius of a typical galaxy radius r times a numerical factor. Since the spectrum of residual light is the Planck's black-body distribution [23], one obtains a prediction for the temperature of the CMB from the Stefan-Boltzmann law.

The observed value of the CMB temperature $T = 2.7\ K$ can indeed be naturally explained. Taking the luminosity of Milky Way, $L = 5 \times 10^{36}\ W/m^2$ for the luminosity of a typical galaxy, our model gives $T = 2.74\ K$. (To give a sense of sensitivity of this prediction to assumed typical luminosity, if one takes the luminosity of Andromeda galaxy ($M31$) as that of a typical galaxy, the model gives $T = 3.2\ K$. We note that Andromeda is a bright galaxy, most likely more luminous than an average galaxy in the universe.)

One can show that the main feature in the CMB power spectrum, the first peak at $l \sim 200$, can be reproduced in this model, as shown In Figure 5. We used a simple model in which galaxies are distributed according to a hierarchical sequence of distances between superclusters, clusters and galaxies, with the distance scales taken from existing observations [45], while keeping the number of galaxies per unit volume on large distance scales uniform. Specific values can be found in Appendix 3. We generated a network of galaxies' positions in the sky, together with their corresponding energy fluxes, taking into account reduction of the flux according to galaxies'

distances from the observer, and their geometrical redshift. The shape of the power spectrum is sensitive to the assumed distance scales between superclusters, clusters, galaxies, and R, the 'radius of the universe'. We used the healpy [46] Python package to convert the sky coordinates to obtain maps of the sky using the NSIDE=512 HEALPix pixelization scheme, and then calculated the power spectra of the simulated fluctuations. This is the same pixelization scheme that was used for WMAP data, which did not have very high angular resolution (0.3-0.96 degrees). We believe this choice was appropriate to explore whether the first peak of the power spectrum can be explained by our very simple, preliminary model. However, higher resolution data is available for future efforts to reproduce higher order characteristics of the power spectrum. More information about the details of our model can be found in Appendix 3.

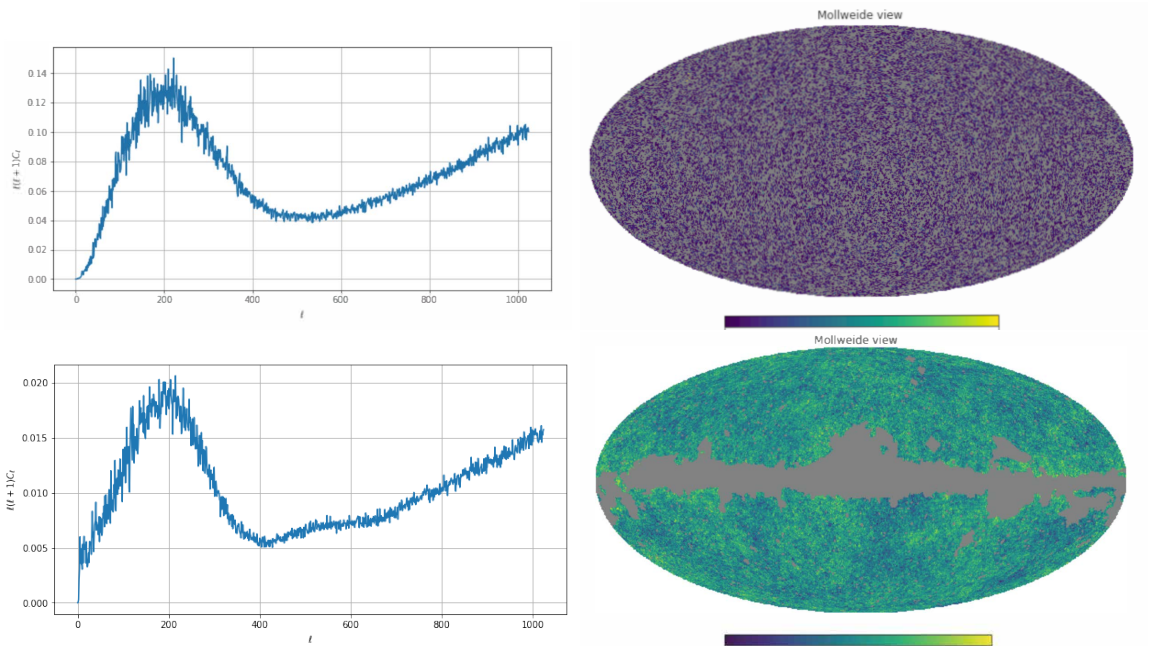

Figure 5: The simulated CMB power spectrum in Einstein-Segal universe (top left) calculated with healpy directly from a sky map of temperature fluctuations generated in Mathematica (top right) assuming a hierarchical distribution of galaxy superclusters, galaxy clusters and voids. The parameter values used in this simulation were: the number of superclusters $N_{\text{supercl}} = 0.1 \times 10^6$; the distance between superclusters $D = 15$ Mps; the number of clusters in a supercluster $N_{\text{cl}} = 20$; the number of galaxies in a cluster $N_{\text{g}} = 20$ and the 'radius of the universe' $R = 600$ Mps. More details about the range of parameters used in our model can be found in Appendix 3. For comparison, the corresponding CMB power spectrum calculated directly from WMAP is shown (bottom left) together with a WMAP data showing CMB temperature in our universe.

3 Conclusion

Segal's 'Chronometric Cosmology', in which the geometry of the universe is spatially closed, finite and eternal, provides an alternative explanation for cosmological redshift, and provides a verifiable prediction on the redshift-

distance dependence. We have compared the predictions of the Standard Model of Cosmology and Segal's universe cosmology with data on cosmological redshift, specifically $m(z)$ and $N(< z)$, and with the temperature and power spectrum of the CMB. Surprisingly, the data is consistent with predictions of Segal's $M = \mathbb{R} \times \mathrm{S}^3$ universe.

We believe further research is merited into Segal's Chronometric Cosmology model. Following a more detailed investigation of the consistency of observational data with alternative models of the universe, future work should explore the questions of conservation of energy, creation of matter, and whether the distribution of elements observed in our universe could be explained in a spatially closed, static and eternal Segal-Einstein universe.

Additionally, the next few years will continue to bring more data from the already operational James Webb Space Telescope, which will extend the reach and the resolution of studies of distant galaxies and objects at high redshifts. A dedicated study of the $N(< z)$ relation for chosen fixed angular cones in one of the Deep Fields could provide important information about the geometry of the universe. The James Webb Space Telescope data could also provide important information about extinction and absorption of light emitted by distant sources, and the evolution of stars and galaxies in time, which at present introduce complications to the interpretation of both $m(z)$ and $N(< z)$ studies.

ACKNOWLEDGMENT

We would like to thank Loring Tu for discussions, comments and a careful reading of the manuscript.

Appendix 1:

Compactification of $\mathbb{R} \times \mathbb{R}^3$ as projective quadric in a 6-dimensional Euclidean space with $(2, 4)$ signature

One can compactify the Minkowski space M_0, with $\mathrm{O}(1, 3)$ as its symmetry group, by including it into the projective light cone (i.e. the space of all null lines through the origin) in a 6-dimensional Euclidean space $\mathbb{R}^4 \times \mathbb{R}^2$ with (2,4) signature [13]. The group $\mathrm{SO}(2, 4)$ naturally acts on this space.

Given Cartesian coordinates $(x^0, x^1, x^2, \cdots x^{n-1}, k, q) \in \mathbb{R}^n \times \mathbb{R}^2$, with $k \neq 0$, one can define a new set of

coordinates $(y^0, y^1, \cdots y^{n-1}, y^n, y^{n+1})$ by

$$\begin{cases} y^\mu = x^\mu k, \quad \mu = 0, \cdots n-1 \\ y^n = (q+k)/2 \\ y^{n+1} = (q-k)/2. \end{cases} \tag{4}$$

The inverse transformation is

$$\begin{cases} x^\mu = y^\mu/k, \quad \mu = 0, \cdots n-1 \\ k = y^n - y^{n+1} \\ q = y^n + y^{n+1} \end{cases} \tag{5}$$

If the metric on $\mathbb{R}^n$ is Lorentzian,

$$(x, x) = (x^0)^2 - (x^1)^2 - (x^2)^2 - \cdots - (x^{n-1})^2, \tag{6}$$

the associated quadratic form on $\mathbb{R}^n \times \mathbb{R}^2$ is

$$Q(y, y) = (y^0)^2 + (y^{n+1})^2 - (y^1)^2 - (y^2)^2 - \cdots - (y^n)^2. \tag{7}$$

For Minkowski space $n = 4$. The associated projective space of $\mathbb{R}^4 \times \mathbb{R}^2 = \mathbb{R}^6$ is

$$\mathbb{RP}^5 = (\mathbb{R}^6 \setminus \{0\})/\sim, \tag{8}$$

where two non-zero vectors $v, w \in \mathbb{R}^6 \setminus \{0\}$ are equivalent if there is a non-zero number $\lambda \in \mathbb{R} \setminus \{0\}$ such that $\lambda v = w$. Denote by $[y^0, y^1, y^2, y^3, y^4, y^5]$ the equivalence class of $y^0, y^1, y^2, y^3, y^4, y^5$ on $\mathbb{R}^6 \setminus \{0\}$. The equation $y^4 = y^5$ defines a hyperplane H in $\mathbb{RP}^5$, called the hyperplane at infinity. The equation $Q(y, y) = 0$ defines a quadric Z of dimension 4 in $\mathbb{RP}^5$

$$Q(y, y) = (y^0)^2 + (y^5)^2 - (y^1)^2 - (y^2)^2 - (y^3)^2 - (y^4)^2 = 0. \tag{9}$$

The points of Z not lying on H are diffeomorphic to Minkowski space M_0 and the quadric Z is its compactification. The quadric Z remains invariant under the action of $\mathrm{SO}(2, 4)$ group. The group of causal conformal transformations on $\mathbb{R}^4 \times \mathbb{R}^2$ are those for which $Q(y, y) = 0$. Because the coordinate sets $(y^0, y^1, y^2, y^3, y^4, y^5) \simeq \lambda(y^0, y^1, y^2, y^3, y^4, y^5)$ are equivalent up to a multiplicative factor λ with points in Minkowski space M_0, one can rewrite $Q(y, y) = 0$ as

$$(y^0)^2 + (y^5)^2 = (y^1)^2 + (y^2)^2 + (y^3)^2 + (y^4)^2 = 1. \tag{10}$$

Thus the compactified Minkowski space on which the conformal group acts continuously is compact and topologically isomorphic to $\overline{M} \simeq (\mathrm{S}^1 \times \mathrm{S}^3)/\mathbb{Z}_2$, or that time is compactified to S^1 and space to S^3. Time becomes periodic. To avoid this, one has to use the universal covering space $M \simeq \mathbb{R} \times \mathrm{S}^3$.

The manifold $\widetilde{M} = \mathrm{S}^1 \times \mathrm{S}^3$ is the two-fold covering space of $\overline{M}$, while $M = \mathbb{R} \times \mathrm{S}^3$ covers it infinite number of times. The Minkowski space M_0 can thus be regarded as an open dense submanifold of $\overline{M}$ which is covered infinitely many times by M. The space $\mathrm{S}^1 \times \mathrm{S}^3$ admits a local notion of causality, but it not causal globally. The space $\mathbb{R} \times \mathrm{S}^3$ is the universal covering space of the conformal compactification $\overline{M}$ of Minkowski space M_0 which is globally causal [13].

Compactification of $\mathbb{R} \times \mathbb{R}^3$ as a manifold with a U(2) group action

Minkowski space M_0 can also be compactified as the group manifold of the unitary group U(2) via the Cayley transform. Minkowski spacetime can be represented by the causally isomorphic real linear space $H(2)$ of 2×2 Hermitian matrices. For a point $P \in M_0$ with coordinates $(x^0 \coloneqq ct, x^1, x^2, x^3)$, with c the speed of light, the corresponding matrix A is:

$$\mathrm{A} = \begin{pmatrix} x^0 + x^3 & x^1 + \mathrm{i}x^2 \\ x^1 - \mathrm{i}x^2 & x^0 - x^3 \end{pmatrix} \in H(2)$$

This defined a map $\alpha : M_0 \to H(2)$. The vector space $H(2)$ of 2×2 Hermitian matrices can be causally immersed as a dense subset of the compact group U(2) of 2×2 unitary matrices as follows. For a Hermitian matrix A, the Cayley transform U(A) is the corresponding matrix:

$$\mathrm{U(A)} = (\mathbb{I} + \tfrac{1}{2}\mathrm{iA})(\mathbb{I} - \tfrac{1}{2}\mathrm{iA})^{-1} \tag{11}$$

where $\mathbb{I}$ is the identity matrix. The Cayley transform, $\beta : H(2) \to \mathrm{U}(2), \mathrm{A} \mapsto \mathrm{U(A)}$, is one-to-one and, importantly, causal. It has a unique inverse, which is the generalized stereographic projection,

$$\mathrm{A} = -2\mathrm{i}(\mathrm{U} - \mathbb{I})(\mathrm{U} + \mathbb{I})^{-1}, \tag{12}$$

well defined as long as $\det(\mathrm{U} + \mathbb{I}) \neq 0$. The generalized stereographic projection is an analogue of the mapping between the unit circle in the complex plane, a multiplicative Lie group, and the imaginary axis its Lie algebra. The conformal infinity is the subset of U(2) consists of those matrices $\mathrm{U} \in \mathrm{U}(2)$ for which $\det(\mathrm{U} + \mathbb{I}) = 0$.

The group SU(2, 2) acts on U(2) via the map $\rho(T) : \mathrm{U} \to (A\mathrm{U} + B)(C\mathrm{U} + D)^{-1}$, which, for any $T = \begin{pmatrix} A & B \\ C & D \end{pmatrix} \in \mathrm{SU}(2,2)$, is a homomorphism of SU(2, 2) into the group of all causal morphisms of U(2).

The compactification U(2) of $H(2)$ can be lifted to its universal covering space $M = \mathbb{R} \times \mathrm{S}^3$. The group SU(2) is isomorphic to unit quaternions and is thus diffeomorphic to S^3, and $\mathrm{U}(2) \simeq \mathrm{U}(1) \times \mathrm{SU}(2)$. More precisely, the quotient U(2)/SU(2) is isomorphic to U(1). The group SU(2) is diffeomorphic to S^3, thus $\mathrm{U}(2) \simeq \mathrm{S}^1 \times \mathrm{S}^3$. Since Minkowski spacetime is isomorphic to $H(2)$, it follows that $\mathbb{R} \times \mathrm{S}^3$ is the covering space of the compactification of

Minkowski spacetime, $\mathbb{R}\times\mathbb{R}^3$. The following sequence of mappings [35] causally immerses Minkowski spacetime M_0 into the Segal-Einstein universe M:

$$M_0=\mathbb{R}\times\mathbb{R}^3\overset{\alpha}{\to}H(2)\overset{\beta}{\to}\mathrm{U}(2)\overset{\sim}{\to}\mathbb{R}\times\mathrm{SU}(2)=\mathbb{R}\times\mathbb{S}^3=M. \tag{13}$$

Appendix 2: Fits to $m(z)$ relations

In Figure 1, plotted are observed magnitudes as a function of redshift for the SCP 'Union2.1' SN Ia compilation data. The SCM prediction for $m(z)$, has been evaluated with the expression derived by Sandage [37], equation 33, page 577:

$$m_{\mathrm{bol}}(z)=M_0+5\log_{10}(\frac{1}{q_o^2}(zq_o+(q_o-1)(-1+\sqrt{2q_oz+1})))+C \tag{14}$$

where $C=2.5\log_{10}(4\pi)+5\log_{10}(\frac{c}{H_o})$, with speed of light c and Hubble constant H_o. The parameter q_o was set to the value of $\frac{1}{2}$ for a flat universe and M_{bol}, the absolute brightness, was included with C as a free parameter. In addition, we included in the fit a correction for the observed intensity to account for possible extinction, $I_{\mathrm{corr}}=I\mathrm{e}^{-\lambda c\tau}$, which gives an additional term $2.5\lambda\log_{10}(1+z)$ in the expression for $m_{\mathrm{bol}}(z)$, where λ is the extinction coefficient, a free parameter.

The prediction of Segal's for $m(z)$ has been obtained using the expression given by Segal [13] on page 94:

$$m(z)=2.5\log_{10}z-2.5(2-\alpha)\log_{10}(1+z)+C \tag{15}$$

where α is the power in the spectral function $f(\nu)\propto 1/\nu^{\alpha}$, where ν is the frequency. The parameter α was set to 1. Setting α to some other value, say 2-3, gives almost identical results, except for a different value for the parameter λ, which is adjusted by the fit while leaving the fit quality almost identical. We also included in the fit a correction for the observed intensity to account for possible extinction, which results in an additional term $5\lambda\log_{10}(\mathrm{e})\tan^{-1}(z^{1/2})$ in the expression for $m(z)$. The two fits have the same number of free parameters. Both fits are good, the values of χ^2/dof, reported by Mathematica are 0.98 for SCM and 1.67 for Segal's model, where dof—the number of degrees of freedom in the fit.

In Figure 3, plotted are the observed magnitude as a function of redshift for objects from two ASTRODEEP Frontier Fields, Abell-2744 and MACS-J0416. The curves shown in this figure are based on results of fits obtained with Standard Cosmological Model [37] (red) and Segal's $\mathbb{R}\times\mathrm{S}^3$ (green) and extrapolated to a wider redhift range. We have used the same parameters as obtained in fits to the SCP 'Union2.1' supernovae data shown in Figure 1, except for an additive constant. Both curves describe the data well, however results are inconclusive.

For the fits to Abell-2744 field data, the values of χ^2/dof reported by Mathematica are 2125.71 for SCM and 2092.68 for Segal's model.

Appendix 3: CMB temperature and the first peak in the CMB power spectrum

In Segal's model the CMB corresponds to 'residual light', light that has not been absorbed over many turns around the universe. Following Segal's original approach, the absorption coefficient α is the fraction of the sky blocked by the randomly distributed N galaxies in S^3, each with radius r. The 4-dimensional analogue of the polar angle in S^3, at which all N galaxies should be placed to result in the same absorption coefficient as if they were uniformly distributed in S^3 space, is $\rho_{\text{eff}} = \pi/4$, or $\rho = 3\pi/4$. Since $\rho = l/R$, and $a = R\sin\rho$, it follows that the effective radius a_{eff}, the radius of a slice of S^3 at which one may place all N galaxies to give the same absorption, is

$$a_{\text{eff}} = R\sin(\pi/4) = R\sin(3\pi/4) = R/\sqrt{2}. \tag{16}$$

The absorption coefficient α can be thus estimated by finding the ratio of areas obscured by N galaxies to the area of a slice of S^3 of the radius a_{eff}, or the area of a slice of S^3 at effective 4D polar angle ρ_{eff}:

$$\alpha = N\pi r^2/(\pi R^2(1 - \cos^2\rho_{\text{eff}} + \sin^2\rho_{\text{eff}}) \tag{17}$$

$$\alpha = N\pi\epsilon^2/(\pi(1 - \cos^2(\pi/4) + \sin^2(\pi/4)) = N\pi\epsilon^2/(\pi(1 - \cos^2(\pi/4) + \sin^2(\pi/4)) \tag{18}$$

which gives $\alpha = \epsilon^2 N/2$, where $\epsilon = r/R$.

As described in the main text, $\alpha \ll 1$ and the total energy flux of light that has not been absorbed over n half-turns is $Pe^{-\alpha n}$, where P is the energy flux of 'pristine' light. Summing a resulting power series gives

$$P_{\text{CMB}} = \sum_{n=1}^{\infty} P\mathrm{e}^{-\alpha n} = P/\alpha \tag{19}$$

To calculate the average flux of pristine light at a typical point of the S^3 universe, or the energy flux Φ emitted by N galaxies of luminosity L, randomly distributed in S^3 universe, we used the effective distance $a_{\text{eff}} = Rsin\rho_{\text{eff}}$ at which all N galaxies should be placed to give the same flux $\rho = \pi/4$ or $\rho = 3\pi/4$.

$$\Phi = NL/(4\pi a^2) = NL/(2\pi R^2(1 - \cos(\pi/4)^2 + \sin(\pi/4)^2)) = NL/(2\pi R^2) \tag{20}$$

P is the energy flux of 'pristine' light, emitted by N galaxies distributed uniformly in the universe, averaged over the entire universe and taking redshift into account. The observed energy flux of the pristine light will be reduced by the redshift z. In Segal's model, after integration over the entire space, $\Phi_{\text{corr}} = P/2$. The luminosity

of a typical galaxy L can be estimated from the energy flux of pristine light observed on Earth from Milky Way Φ_E, $L = \phi_E 4\pi(r/2)^2$, where we took $r/2$ for the distance from Earth to Milky Way center. The expected flux of CMB is thus the product of corrected energy flux of pristine light at a typical point of the universe and the enhancement factor $1/\alpha$,

$$P_{\rm CMB} = \Phi_{\rm corr}/\alpha = NL/(2\pi R^2)/(\epsilon^2 N/2)/2 = N(\Phi_E 4\pi(r/2)^2)/(2\pi R^2)/(\epsilon^2 N/2)/2 = \Phi_E/2 \tag{21}$$

Alternatively, one can take various estimates of luminosity of Milky Way, or Andromeda, and use their distance from Earth to find the flux observed on Earth. For Andromeda, the expressions will be modified by the ratio of its distance from Earth to the distance from Earth to the center of Milky Way. We obtained the temperature of a black body corresponding to the predicted energy flux $P_{\rm CMB}$ using Stefan-Boltzmann law: $T = (P_{\rm CMB}/\sigma)^{1/4}$, where σ is the Stefan-Boltzmann constant.

The power spectrum for CMB characterizes two-point correlations between fluctuations of CMB temperature measured in pixels according to a scheme defined in the healpy package. For the WMAP data, which detector had limited angular resolutions, the number of pixels was smaller than for Planck data. We used the same pixelization scheme to compare with WMAP, to allow a comparison of main features of the power spectrum with our crude model. In our approach, we are adding up the energy flux from all sources, assumed to be galaxies of some typical luminosity, falling into a given pixel. Since we are integrating over the entire volume of S^3 space, and account for the dependence of the flux on the distance from the observer, this method provides an estimate of the average energy flux of 'pristine light' in the universe. This flux is related to the energy flux of CMB. In Segal's model, CMB is the 'residual light', not absorbed over many turns. It is larger than the average flux of pristine light by a factor $1/\alpha$, where $\alpha \ll 1$ is the absorption coefficient, as described in the main text. However, the flux of pristine light a typical point of the universe is smaller than the flux of pristine light on Earth, as Earth is located very close to the center of Milky Way. This 'dilution' factor is calculated similarly to the enhancement factor. As a result, and since many factors cancel out, the CMB flux in Segal's model is expected to be the product of some numerical factor f and the energy flux from a typical galaxy at a chosen distance from an observer.

To generate the power spectrum we used a crude simulation with the number of superclusters $N_{\rm supercl} \sim (0.1 - 0.5) \times 10^6$, the number of clusters in a supercluster $N_{\rm cl} = 10 - 20$, the number of galaxies in a cluster $N_{\rm g} \sim 20 - 30$, and the 'radius of the universe' $R > 300 - 800$ Mps. The distance between superclusters was assumed to be $D \sim 10 - 30$ Mps, and this value was taken as the 'thickness' of S^3 slices, surfaces of spheres S^2 of varying radii a. The distances between galaxy clusters and galaxies were obtained by scaling D by $1/N_{\rm cl}$ and

$1/N_{\rm g}$, correspondingly. The number of superclusters in each slice was taken such that the density of superclusters per unit volume was kept approximately constant. In each slice of S^3, we used Mathematica [47] to generate the supercluster positions on the spheres of radii corresponding to a given slice of S^3. The cluster positions were then distributed randomly on a spherical surface surrounding the generated supercluster positions, using a typical distance between clusters as the appropriately smaller radius. Finally, galaxies were randomly generated around he position of clusters to which the galaxies belonged. Each generated galaxy has been assigned three coordinates (ρ, θ, ϕ), which allows to account for geometric effects and to calculate the energy flux reaching the observer, including those of the redshift. To generate a projection on the 'celestial sphere' we kept the two angular coordinates, (θ, ϕ), after converting them to the galactic coordinates.

Segal proved that the energy spectrum of light circulating multiple times around the universe will be a black-body spectrum [23]. The total energy flux of the simulated pristine light falling into a given pixel, multiplied by the factor f, gives the expected energy flux of CMB in a given pixel. Taking the fourth root of the simulated CMB energy flux gives the temperature T of a black body that would give the same energy flux. In this way we obtained a simulated pixelized map of CMB temperature. Finally, we used the healpy package to obtain the power spectrum of the fluctuations of pixel temperatures.

The range of values that seem to reproduce the first peak in the CMB power spectrum at $l \sim 200$ is quite wide, it is the ratios of the distance scales that are important. However, the sensitivity of the position of the first peak in the CMB power spectrum to R opens a possibility, in principle, to estimate the range of values of R allowed by the CMB data.

References

[1] E. Hubble, A Relation between 'Distance and Radial Velocity among Extra-Galactic Nebulae', Contributions from the Mount Wilson Observatory, Carnegie Institution of Washington, 310 1, (1927), and Proc.Nat.Acad.Sci. 15 (1929) 168-173

[2] Edwin Hubble and Richard C. Tolman, 'Two Methods of Investigating the Nature of the Nebular Red-shift', The Astrophysical Journal **82** (1935), pp. 302-337

[3] I. Segal, 'Covariant Chronogeometry and Extreme Distances'. I, Astron. and Astrophys. **18** (1972) 143

[4] Aubert Daigneault and Arturo Sangalli, 'Einstein's Static universe: An Idea Whose Time Has Come Back?', Notices of the AMS, Vol. **48**, number 1, January 2000

[5] A.H. Taub, book review of: 'Mathematical cosmology and extragalactic astronomy', by Irving Ezra Segal, Pure and Applied Mathematics, vol. 68, Academic Press, New York, 1976, Bulletin of the American Mathematical Society, Volume **83**, Number 4, July 1977.

[6] I. Segal, 'A class of operator algebras which are determined by groups', Duke Math. J . 18, (1951) 221.

[7] I. Segal, 'Positive-energy particle models with mass splitting',. Proc. Nat. Acad. Sci. U.S.A. 57, (1967) 194.

[8] I. Segal, 'Causally oriented manifolds and groups', Bull. Amer. Math. Soc. Vol. 77, number 6, (1971) 958

[9] Irving Segal,'Causally connected manifolds and groups', Bull. Amer. Math. Soc. **77** (1971) 958

[10] I. E. Segal, 'A Variant of Special Relativity and Long-Distance Astronomy', Proc. Nat. Acad. Sci., **71** (1974) 765

[11] I. E. Segal,'Observation validation of the chronometric cosmology: I. Preliminaries and the redshift-magnitude relation', Proc. Nat. Acad. Sci., **72** (1975) 2273

[12] J. F. Nicoll and I. E. Segal,'Phenomenological analysis of the observed relations for low-redshift galaxies', Proc. Nat. Acad. Sci., **72** (1975) 2273

[13] I. E. Segal,'Mathematical Cosmology and Extragalactic Astronomy', Academic Press, New York, 1976, Pure and Applied, Vol. 68

[14] I. E. Segal,'Theoretical foundations of chronometric cosmology', Proc. Nat. Acad. Sci., **73** (1976) 669

[15] I. E. Segal, 'Interacting quantum fields and the chronometric principle', Proc. Nat. Acad. Sci., **73** (1976) 3355

[16] Edward E. Fairchild, 'The Segal Chronometric Redshift - A Classical Analysis', Astron. and Astrophys. **56** (1977) 199

[17] I. E. Segal, 'Correction to Erroneous Presentation of Chronometric Redshift Theory', Astron. and Astrophys. **68** (1978) 343

[18] I. E. Segal, 'Some resent tests of the chronometric cosmology', Proc. Nat. Acad. Sci., **77** (1980) 10

[19] I. E. Segal, 'Time, energy, relativity and cosmology', in Symmetries in Science, B. Gruber et. al. (eds), Chapter 10, page 385, Plenum Press, New York, 1980

[20] Stephen M. Paneitz and Irving E. Segal, 'Analysis in Space-Time Bundles. I. General Considerations and the Scalar Bundle', J. Funct. Anal , **47** (1982) 457

[21] Stephen M. Paneitz and Irving E. Segal, 'Analysis in Space-Time Bundles. II. The Spinor and Form Bundles', J. Funct. Anal , **49** (1982) 335

[22] Stephen M. Paneitz and Irving E. Segal, 'Analysis in Space-Time Bundles. III. Higher Spin Bundles', J. Funct. Anal , **54** (1983) 18

[23] I. E. Segal, 'Radiation in the Einstein universe and the cosmic background', Phys. Rev. D. **28** (1983) 2393

[24] I. E. Segal, 'Evolution of the Inertial Frame of the universe', Nuovo Cimento B **79** (1984) 187

[25] Laurence I. Wormald, 'A Critique of Segal's Chronometric Theory', Gen. Relativ. Gravit. **16** (1984) 393

[26] I. E. Segal, 'Concerning - A Critique of Segal's Chronometric Theory, by Laurence I. Wormald', Gen. Relativ. Gravit. **16** (1984) 403

[27] I. E. Segal, 'The redshift-distance relation', Proc. Nat. Acad. Sci., **90** (1993) 4798

[28] I. E. Segal, 'Geometric derivation of the chronometric redshift', Proc. Nat. Acad. Sci., **90** (1993) 11114

[29] I. E. Segal and Z. Zhou, 'Convergence of quantum electrodynamics in a curved modification of Minkowski space', Proc. Nat. Acad. Sci., **91** (1994) 962

[30] I. E. Segal and Z. Zhou, 'Maxwell's equations in the Einstein universe and chronometric cosmology', Astrophys. J. Suppl., **S 100** (1995) 307

[31] Irving Segal and Zhengfang Zhou, 'Conformal Extension of Massive Wave Functions', J. Funct. Anal , **155** (1998) 550

[32] I. E. Segal, 'Cosmological implications of a large complete quasar sample', Proc. Nat. Acad. Sci., **95** (1998) 4804

[33] I. E. Segal, 'Is redshift-dependent evolution of galaxies a theoretical artifact?', Proc. Nat. Acad. Sci., **96** (1999) 13615

[34] I. E. Segal and J. F. Nicoll, 'Astronomy phenomenological analysis of redshift-distance power laws', Astrophys. Space Sci., **274** (2000) 503

[35] Aubert Daigneault, 'Irving Segal's Axiomatization of Spacetime and its Cosmological Consequence', Invited lecture given at the conference celebrating the 100th anniversary of the Hungarian mathematical logicians László Kalmár and Rózsa Péter in Budapest, August 5, August 11, 2005

[36] Alexandrov, A.D. and Ovchinnikova, V.V., 'Notes on the foundations of relativity theory', Vestnik Leningrad Univ., 11 (1953), 95. ; Zeeman, E.C., 'Causality implies the Lorentz group', Journal of Mathematical Physics, 5, (1964) 490-493

[37] A. Sandage, 'Observational Tests of World Models', Annual Review of Astronomy and Astrophysics 26.1 (1988) p. 561-630

[38] Carroll, Sean M. ; Press, William H. ; Turner, Edwin L., 'Cosmological Constant'. Annual Rev. Astron. Astrophys., Vol. 30, p. 499-542 (1992)

[39] Suzuki et al (The Supernova Cosmology Project): 'The Hubble Space Telescope Cluster Supernova Survey: V. Improving the Dark Energy Constraints Above $z > 1$ and Building an Early-Type-Hosted Supernova Sample', ApJ **746**, 85 (2012)

[40] M. Castellano at al., 'The ASTRODEEP Frontier Fields Catalogues: II - Photometric redshifts and rest-frame properties in Abell-2744 and MACS-J0416', Astron. & Astrophys. **590** (2016) A31

[41] Gardner, J.P., Mather, J.C., Clampin, M. et al. 'The James Webb Space Telescope'. Space Sci Rev 123, 485-606 (2006). https://doi.org/10.1007/s11214-006-8315-7

[42] Labbé, I. et al., 'A population of red candidate massive galaxies ∼600 Myr after the Big Bang'. Nature. **616**, 266 (2023)

[43] Carniani, S et al., 'A shining cosmic dawn: spectroscopic confirmation of two luminous galaxies at $z \sim 14$'. arXiv:2405.18485 [astro-ph.GA]

[44] https://lambda.gsfc.nasa.gov/education/graphic_history/microwaves.html

[45] https://en.wikipedia.org/wiki/List_of_largest_cosmic_structures,https://en.wikipedia.org/wiki/Supercluster, https://en.wikipedia.org/wiki/Void_(astronomy)

[46] A. Zonca et al., 'healpy: equal area pixelization and spherical harmonics transforms for data on the sphere in Python', The Open Journal vol 4, 35 (2019) 1598; K. M. Gorski et al.: 'HEALPix: A Framework for High-Resolution Discretization and Fast Analysis of Data Distributed on the Sphere', Astrophys.J vol **622** (2005) 759

[47] Wolfram Research, Inc., Mathematica, Version 14.0, Champaign, IL (2024).